Theory of X^- at high magnetic fields

D. M. Whittaker and A. J. Shields
Toshiba Cambridge Research Centre, 260 Cambridge Science Park, Milton Road, Cambridge CB4 4WE, United Kingdom
(Received 18 April 1997; revised manuscript received 5 June 1997)

We calculate, to high accuracy, the states of the quantum-well negatively charged exciton X^- in a perpendicular magnetic field. Two GaAs structures are considered: a 100-Å ''narrow'' well and a 300-Å ''wide'' well. The calculations cover a magnetic field range from 5 T to 50 T. In the narrow well, the ground state is shown to switch from singlet to triplet, at about 30 T, in agreement with the prediction of a triplet ground state obtained using the lowest-Landau-level approximation. In the wide well, the singlet is still the ground state at 50 T because electron-hole correlations perpendicular to the well plane enhance its binding energy more than that of the triplet. We also calculate electron-electron correlation functions for the X^- states and demonstrate that in the singlet the motions of the two electrons are correlated, while in the triplet they are anticorrelated. We show that the triplet binding energies in the wide well are in good agreement with experimental data; the singlet values, however, turn out to be considerably smaller than those measured. [S0163-1829(97)03347-X]

I. INTRODUCTION

The idea of a negatively charged exciton, or X^-, was introduced by Lampert[1] as the semiconductor analog of the negatively charged hydrogen atom H^-. The X^- consists of two electrons and a hole, which are bound together by their mutual Coulomb interactions. Recent interest in the two-dimensional realization of this system has followed the observation of X^- features in the spectra of high-quality remotely doped GaAs quantum wells by Shields *et al.*[2] and Finkelstein *et al.*[3] The behavior of the quantum well X^- in electric[4] and magnetic fields[5] has subsequently been studied and it is the latter that we investigate theoretically in the present paper.

The X^- can be thought of as a neutral exciton $X^0$with a second electron bound to it. The binding energy of the first electron to the hole, forming X^0, is fairly large, ~ 8 meV in a typical GaAs quantum well. The second electron binds by polarizing the X^0 to produce a dipole. The interaction between the electron and this dipole is weak, so the second electron binding energy is much less, typically ~ 1 meV.

This description of X^- is inaccurate in that it suggests that the two bound electrons are distinguishable. In fact, they are identical, so a proper picture must include the antisymmetry of the state when the electrons are exchanged. The role of exchange for the two electrons is the same as in the textbook example of the He atom: The wave function factorizes into a spatial part and a spin part, which can have either total $S=0$ (singlet) or $S=1$ (triplet). The singlet state is antisymmetric under the exchange of spins, so to retain the correct overall antisymmetry of the wave function, the spatial part must be symmetric. The triplet, by contrast, is symmetric, so the corresponding spatial part must be antisymmetric.

For the He atom, the strong electron-nucleus interaction dominates the electron-electron repulsion, which can thus be treated as a perturbation. The atomic states are described by the single-particle quantum numbers of the two electrons, with the singlet and triplet components of each such configuration split by the exchange contribution to the perturbation energy shift. The triplet always has the lower energy of the two spin states because the antisymmetry of the spatial part of the wave function keeps the two electrons apart and reduces the Coulomb repulsion. This observation is codefied as one of Hund's rules, though it should be noted that there are important exceptions, including the ground state of the He atom, which is a singlet. The ground-state configuration consists of two electrons in the same spatial state, so only the symmetric singlet combination, with opposing spins, is allowed. In fact, it can be shown rigorously that the ground state of any two-electron ''atom,'' including X^-, is necessarily a singlet in the absence of a magnetic field.[6]

X^- is rather different from He because the hole carries only one unit of positive charge, making the contributions of the electron-electron and electron-hole interactions much more comparable. The perturbative description given above is no longer appropriate, though the classification of states as singlets or triplets is, of course, still rigorous. In the two-dimensional X^-, only the singlet ground state is bound without a magnetic field. This bound state has been investigated by a number of authors, using variational[7] and quantum Monte Carlo methods.[8,4]

When a magnetic field is applied, the net charge on X^- causes its center-of-mass motion to be quantized into Landau levels.[9] This contrasts with the behavior of the center of mass of the neutral X^0, which does not ''feel'' the magnetic field directly and so has a continuous dispersion. The quantization causes the X^- states to be highly degenerate (see Sec. III below). At fields greater than a few tesla, a second, triplet, bound state appears.[5] This happens because the Landau-level degeneracy means that the Pauli principle no longer provides such a strong constraint as at zero field. Indeed, at very high fields, it is generally believed that the triplet should, in accordance with Hund's rules, become the ground state. Our calculations confirm this, but only in narrower wells and then only at fields greater than 30 T.

Although there is a large literature on the D^- system, two electrons bound to a positive donor, relatively little work has been done on X^-. Despite the superficial similarities of the two systems, their behavior is both qualitatively and quantitatively very different, as we discuss in Sec. III, so separate calculations are required. Previous studies of X^- binding en-

ergies in magnetic fields, by Stébé *et al.*,[9,10] have concentrated on the low-field regime, using variational wave functions. They are exactly two dimensional, taking no account of the effects of finite well width. The only published high-field calculations use a restricted basis of lowest-Landau-level states,[11,12] which gives unrealistic results for the fields of interest experimentally: Though the triplet state is reasonably well described, the singlet is predicted to be unbound, while in fact it is the ground state. The calculations we present are for the high-magnetic-field regime, with fields in the range 5–50 T. Though a finite basis of single-particle electron and hole states is used, careful attention is paid to ensure good convergence with respect to the basis size. The calculations take into account the effects of a finite well width, through both the modification of the in-plane Coulomb interaction and the inclusion of states from higher subbands in the basis. The higher subband states are particularly important for the 300-Å quantum well, as they allow for correlations perpendicular to the well plane.

The layout of the remainder of the paper is as follows. Section II gives an outline of the calculation. Sections III and IV discuss the numerical results, both approximate and exact. Section V describes the wave functions of the X^- states and Sec. VI compares our theoretical binding energies with experimental results for a 300-Å GaAs quantum well. Appendices A and B give technical details of some of the more important results used in the numerical work.

II. CALCULATION

Our model consists of a finite-width quantum well, with finite barriers and parabolic conduction and valence bands. Details of the material parameters used are given in Appendix A. The magnetic field is perpendicular to the quantum well and the symmetric gauge $\mathbf{A}=(\mathbf{B}\times\mathbf{r})/2$ is chosen so that angular momentum M is a good quantum number. This section describes the analytic and numerical methods we use to obtain the X^- states using this model.

The major difficulty in any X^- calculation lies in the large numbers of degrees of freedom that the system posseses. There are three spatial coordinates for each of the three particles, giving a total of nine. Without a magnetic field, it is relatively easy to simplify the problem making use of the in-plane translational invariance to separate out the center-of-mass motion.[7] In a magnetic field, this separation is still possible, but the Hamiltonian becomes complicated, with terms coupling the relative and center-of-mass parts. However, this approach was followed by Stébé *et al.*[9,10] for their low-field work, using variational wave functions.

For high fields, the most practical way to proceed is to work in a basis of single-particle electron and hole states, which are eigenstates in the absence of the Coulomb interaction. The electron-electron and electron-hole interactions are then diagonalized within this basis. The basis states are products of an axial (z) part, determined by the quantum-well confinement, and an in-plane (r,θ) Landau-level wave function. For electrons, the basis states take the form

$$|lnm\rangle=\chi_l(z)\ \phi_{nm}(r)\ e^{i(n-m)\theta}. \tag{1}$$

This state is degenerate with respect to the azimuthal quantum number m and has energy $E_l+(n+\frac{1}{2})\hbar\omega$. E_l is the confinement energy of the lth quantum well level and $\hbar\omega$ the electron cyclotron energy. The full form of the axial and radial wave functions χ and ϕ are given in Appendix A. For the hole, the quantum-well part χ is generally different, but the in-plane part is just the complex conjugate of the electron wavefunction, which simply switches the sign of the exponent. As a result, electrons and holes with the same quantum numbers have angular momentum of opposite sign: For electrons $M_e=n-m$ and for holes $M_h=m-n$.

The wave function for X^- is expanded as a sum over symmetrized trios of such single-particle states:

$$\psi=\sum_{\{l,n,m\}}\alpha_{\{l,n,m\}}|l_hn_hm_h\rangle\frac{1}{\sqrt{2}}\{|l_1n_1m_1\rangle|l_2n_2m_2\rangle \pm|l_2n_2m_2\rangle|l_1n_1m_1\rangle\}. \tag{2}$$

The plus sign is taken for the spatially symmetric singlet,[13] while the minus sign applies to the antisymmetric triplet. The notation $\{l,n,m\}$ has been adopted in Eq. (2) as a shorthand for a complete set of nine quantum numbers (l_h,n_h,m_h) for the hole and $(l_1,n_1,m_1),(l_2,n_2,m_2)$ for the two electrons. There are actually eight independent quantum numbers since the total angular momentum $M=(n_1-m_1)+(n_2-m_2)+(m_h-n_h)$ is a constant of motion. A further constant for symmetric wells is the total parity of the X^-, the product of the parities of the χ for the two electrons and the hole. The low-energy states, discussed in the present work, always have even parity because they are made primarily from basis states in the lowest electron and hole subbands.

The basis states described above are coupled together by the Coulomb interactions between the two electrons and between the electrons and the hole. These conserve total angular momentum and are two-particle interactions, so the matrix element is nonzero only if the other particle has the same quantum numbers in both initial and final states. The exchange symmetry of the electrons means that each matrix element has two parts. There is a direct term, which has the same sign for singlet and triplet states, and an exchange term, which has opposite signs. Details of the evaluation of the pair matrix elements are given in Appendix B.

In principle, the X^- eigenstates are obtained by evaluating the Coulomb matrix elements within a basis consisting of a sufficiently large set of $\{l,n,m\}$ and diagonalizing the resulting matrix. However, to obtain the accuracy of the calculations in this paper requires maximum values of $l\sim5$, $n\sim10$, and $m\sim20$. Simplistically taking these as upper limits would give $\sim10^7$ states, entailing the evaluation of an impossibly large number of matrix elements. The actual basis used in the calculations is much smaller, typically a few thousand states, selected because they contribute significantly to the X^- wave function.

The states used are chosen by an algorithm based upon the idea of progressively expanding the basis set by trying new states and then throwing away those that are not important. This works because, though several thousand states are needed to obtain high accuracy, the X^- is reasonably well described by only a few basis states, with $l=0$ and small m and n. Hence a good initial approximation to the X^- eigenstate is obtained by diagonalizing within a relatively small basis. The wave function is then examined and states whose

TABLE I. Convergence of the total binding energy of the $M=0$ singlet state in a 300-Å well at 20 T, as a function of the probability threshold below which basis states are rejected.

Probability threshold	Energy (meV)	Number of basis states
1×10^{-4}	15.778	126
1×10^{-5}	16.248	454
1×10^{-6}	16.544	1633
1×10^{-7}	16.714	5317
1×10^{-8}	16.786	13314

amplitude lies below a threshold are removed from the basis. The eigenstate is improved by systematically adding blocks of new states and repeating the diagonalization and winnowing processes. The order in which new states are tested is rather arbitrary, and in practice unimportant, but it has to be chosen in a way that allows convergence to be monitored.

The key parameter that determines the accuracy of this method is the selection of the threshold below which basis states are rejected. A smaller threshold gives greater accuracy, but increases the number of basis states that have to be treated. Table I shows how the calculated binding energy depends on the probability threshold. For each order of magnitude reduction in the threshold, the number of basis states roughly doubles and the increment to the binding energy due to the additional states halves. This suggests that for the 1×10^{-8} threshold used in most of our calculations, the residual error should be less than 0.1 meV.

The benefit of our method is that, though a similar number of basis states are tested as would be involved in the equivalent large-scale diagonalization, only matrix elements coupling each of these to the few thousand retained states need be evaluated. The disadvantage is that it is not guaranteed to be as accurate: A state rejected early in the process could become more important when some later states have been included. We believe that this is not a serious problem in the present calculation, as is shown by two types of evidence. The first is our ability to reproduce known results, those for the neutral exciton X^0 discussed at the end of this section, and X^- and D^- in the lowest-Landau-level approximation, discussed in Sec. III. The second type of evidence comes from the internal consistency of our algorithm: The same results are obtained, to the convergence accuracy, if basis states are tested in different orders. The comparison of binding energies for different values of total angular momentum, in Sec. IV, is a further demonstration of internal consistency. Beyond this, it should be noted that our calculations retain the variational character of any finite basis calculation: The numerical eigenvalues are always a strict upper limit on the true energy levels.

All the X^- binding energies quoted in this paper are given relative to that of the neutral exciton X^0 plus a free electron, since a state with lower binding energy is unstable and will not be seen experimentally in photoluminescence. The X^0 binding energy is typically 10–20 meV in the well widths and fields of interest here. Relative to this, the X^- binding energy is 1 meV, so to obtain a reasonable accuracy of 10% in this figure, $\sim$0.1 meV, the total binding energy has to be calculated with an error of less than 0.5%.

The X^0 binding energies are calculated using a similar diagonalization procedure to the X^-, though with only two particles the basis set is much smaller. In fact, for the optically active X^0 with zero center-of-mass momentum, there are no terms coupling to the relative motion, so it is convenient to transform to in-plane relative coordinates, further simplifying the calculation. The results agree very well with an independent calculation of the X^0 binding energy, using numerical integration of the radial wave equation.

III. LOWEST-LANDAU-LEVEL APPROXIMATION

The computation of the X^- states is much simpler if the basis space is restricted to the lowest subband (all $l=1$) and the lowest Landau level (all $n=0$). This sort of approximation should be most valid at high fields, where the Landau-level separation is large, so the higher Landau levels contribute relatively little to the X^- wave function. Though it will be shown later that the results obtained are unrealistic for the experimentally applied fields, the lowest-Landau-level (LLL) approximation has been widely used for other problems, such as the quantum Hall effect, and so it is of theoretical interest. In this section we show that our method reproduces known results for X^- and the negatively charged donor system (D^-), within the LLL approximation. We also contrast these two systems, which are superficially very similar, and explain the significant differences in their behavior.

X^- has essentially just one bound state in the LLL. This is a triplet state. For a perfectly two-dimensional system (an infinite well with $d\rightarrow0$) it has a binding energy, relative to X^0, of $0.0544e^2/\varepsilon l_c$, where l_c is the magnetic length and ε the dielectric constant. The present result agrees very well with the value of $0.0545e^2/\varepsilon l_c$ obtained by Palacios *et al.*[12] in a similar exact diagonalization calculation.

In the LLL, there are no singlet states that are bound, relative to X^0. The singlet ground state consists of a free electron and an exciton. Thus the X^- ground state is expected to change from the singlet at zero field to a triplet at high fields. This crossover is consistent with Hund's rules, which predict that the triplet will generally be at lower energy than the singlet. The exception created by the Pauli principle at zero field no longer applies because the degeneracy of the Landau levels means that a triplet state can be formed with two electrons in different angular-momentum states, at no cost in kinetic energy.

An interesting property of the triplet bound state is that it is infinitely degenerate: The same binding energy is found for all values of total angular momentum $M<0$. This degeneracy is shown by the numerical results, but it is a completely general property, not restricted to the LLL or triplet states. It is a result of the requirement of gauge invariance for charged systems with translational invariance. The gauge argument is one that applies to any charged particle, including an electron, and shows that for a given Landau level n the energy cannot depend on the other quantum number that defines the state. Though the result must be true for all gauges, the argument is clearest using the Landau gauge, $\mathbf{A}=(0,Bx,0)$. In this gauge, the value of k_y that is assigned to a state depends on the choice of the origin for the vector potential. For a translationally invariant system, this choice is arbitrary, so k_y can have no physical significance. No mea-

TABLE II. D^- and X^- bound states with different angular momenta M in the lowest-Landau-level approximation for a two-dimensional system. The binding energies are given relative to X^0 or D^0, in units of $e^2/\varepsilon l_c$.

M	D^- singlet	D^- triplet	X^- singlet	X^- triplet
0	0.367			
−1		0.184		0.0544
−2		0.027		0.0544
−3		0.0006		0.0544

surable property of the state, including its energy, can depend on the value of k_y. Hence the states in a given Landau level must be degenerate. The argument applies to the X^- system since its center of mass behaves like a simple charged particle. For a given center-of-mass Landau level, the energies of the X^- states cannot depend on the total angular momentum M.

Superficially, the D^- system appears to be similar to the X^-: It consists of a positive donor ion with two electrons bound to it. However, the bound states of D^- are very different from those of X^-, as can be seen from Table II, which compares the states of the two systems calculated using our algorithm in the LLL for the two-dimensional limit. The D^- results agree very well with those of Fox and Larsen[14] for their case of the positive ion in the same plane as the electrons. The most obvious properties of D^- are that its binding energy is much larger than that of X^- and its ground state is a singlet rather than a triplet. In addition, there are only four

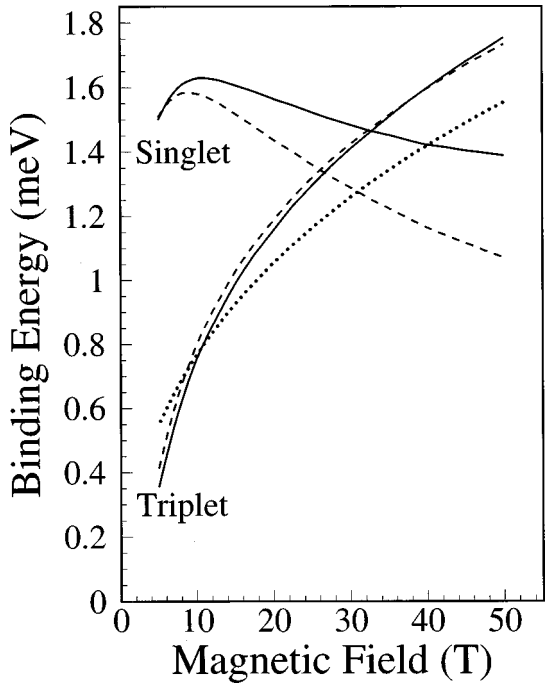

FIG. 1. Binding energies, relative to X^0, of the X^- singlet and triplet states in a 100-Å GaAs/$Al_xGa_{1-x}As$ quantum well, plotted as a function of magnetic field. The various line styles correspond to different approximations for the basis used in the calculations. The dotted lines are for the lowest-Landau-level approximation, the dashed lines for the lowest subband approximation, and the solid lines for the full results.

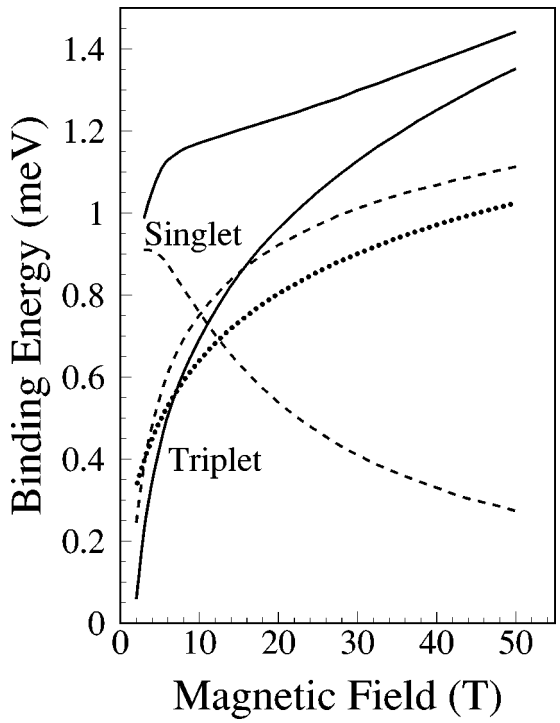

FIG. 2. Binding energies of X^- singlet and triplet states in a 300-Å quantum well, plotted as a function of magnetic field. The meanings of the line styles are the same as in Fig. 1.

nondegenerate bound states of D^-, relative to D^0, while the X^- bound state is infinitely degenerate.

There are two fundamental differences between the X^- and D^- systems, which together account for their contrasting behavior. Both arise from the fact that the hole in X^- is in a Landau level, while the positive ion in D^- is a localized point charge. The first difference is that the hole charge in X^- is spread over a region with a size of the order of the cyclotron radius. As a result, the electron-hole interactions are relatively stronger in D^-, increasing its binding energy and allowing more bound states. Furthermore, as will be shown in Sec. V, stronger electron-hole interactions tend to favor the singlet, which explains why it is the D^- ground state. The second difference is that the fixed donor ion in D^- breaks the translational symmetry discussed above, so the states of different angular momentum are no longer degenerate and only a finite number are bound.

IV. FULL RESULTS

In this section we describe the results of calculations that go beyond the lowest-Landau-level approximation of Sec. III. The basis set is expanded to include both higher Landau levels and higher quantum-well subbands, leading to a realistic model of X^-.

Figures 1 and 2 show calculated binding energies versus field for 100-Å and 300-Å GaAs quantum wells with $Ga_{0.67}Al_{0.33}As$ barriers. Various approximations are used in the calculations and all the energies are given relative to the X^0 energy in the same approximation. The states shown are the lowest-energy singlet and triplet states, calculated with total angular momenta $M=0$ and $M=-1$, respectively. As discussed in Sec. III, there are degenerate states with more

negative M, but it is harder to obtain the same numerical accuracy for them because a larger basis is needed to provide a good description of their wave functions. Hence the numerical results give an erroneous M dependence, but this is small, with less than 0.1 meV variation in the binding energies for values of $M>-5$ at 20 T. To the extent that the calculations for different M are independent, the small size of this variation is a good indication of the convergence of our algorithm.

The dotted lines on the figures correspond to the lowest-Landau-level approximation discussed in Sec. III, but for finite well widths, rather than the two-dimensional results above. The triplet remains the only bound state and it is still degenerate for all $M<0$. The only difference is that the binding energy is no longer proportional to $e^2/\varepsilon l_c$, which would give a $\sqrt{B}$ increase with field. The actual increase is slower, $\sim \ln B$ at high fields, because the axial spread of the wave functions weakens the Coulomb interaction for small electron-hole separations, less than of order the well width. The binding energy is also considerably smaller in the wider well because the weakening of the Coulomb interaction is more significant. This is entirely comparable to the decrease in X^0 binding energies in wide quantum wells.

The dashed lines show the results of calculations in the lowest subband (LSB) approximation, in which the basis set is restricted to the $l=1$ subband, but with full convergence for n and m. The major change, compared to the LLL, is that there is now a bound singlet state in both narrow and wide wells. At low fields, it is the ground state, but as the field is raised its energy rapidly decreases and it falls below the triplet. This decrease is a direct consequence of the singlet being unbound in the LLL, as can be shown using a simple perturbation argument. Consider a two-dimensional system, so all Coulomb matrix elements vary as $\sqrt{B}$. As discussed in Sec. III, in the LLL the X^0 and all X^- binding energies, relative to the Landau-level energy, also increase as $\sqrt{B}$, but with different constants of proportionality α^0 and α^-. Although the singlet is not bound relative to X^0, there is an X^- state at higher energy, so $\alpha^-<\alpha^0$. Now consider the effects of higher Landau levels using second-order perturbation theory. The matrix elements vary as $\sqrt{B}$, but the energy separation, roughly the cyclotron energy, varies as B. Hence in second (and indeed higher) order the B dependences cancel, giving an energy shift β approximately independent of field. Relative to X^0, the singlet binding energy is thus $(\alpha^- - \alpha^0)\sqrt{B}+(\beta^- - \beta^0)$, which *decreases* as $\sqrt{B}$ because $\alpha^-<\alpha^0$. The fact that the singlet is bound in our calculations suggests $\beta^->\beta^0$. This argument predicts that there should be some finite field at which the singlet X^-, within the LSB, unbinds, though that has yet to be reached at 50 T for the systems studied here. The same argument applied to the triplet predicts the binding energy increases as $\sqrt{B}$ because the triplet is bound relative to X^0 in the LLL.

The full lines on Figs. 1 and 2 show the results of the calculations with no restrictions on the Landau levels and subbands contributing to the wave function. They represent our best results for the X^- binding energies. The inclusion of higher subbands allows correlations between the axial coordinates of the three particles to occur since the axial part of the wave function is no longer the same for all terms in the basis.

In the 100-Å well, the triplet energy is almost the same as in the LSB, while the singlet energy is more affected by the inclusion of the higher subbands, particularly at high fields. The difference between the singlet and triplet is a consequence of the relative importance of electron-electron and electron-hole correlations discussed in Sec. V: The singlet binding energy depends on maximizing the electron-hole attraction, while the triplet minimizes the electron-electron repulsion. The most important contributions from the higher subbands come from those of the hole since they are much closer in energy than the electron subbands. Hence including higher subbands allows strong correlations between the electrons and holes to occur in the axial direction, but only weak correlations between the electrons. As a result, the singlet binding energy increases much more than that of the triplet. The increase in importance with field can be readily understood using the same sort of perturbation arguments as have been described above. Just as for the higher Landau levels, the Coulomb matrix elements for the higher subbands increase with field. The subband separation, by contrast, is independent of B, so the overall result is that the second-order terms increase with field.

The difference between the LSB and the full calculations is much more marked for the 300-Å well. When the higher subbands are included, the singlet binding energy actually increases with field, whereas it decreases rapidly in the LSB. The explanation for this is straightforward: The higher subbands are much closer in energy in the 300-Å well than the 100-Å one, so their contributions to the wave function are much greater. The 300-Å well is sufficiently wide to allow some axial correlations between the two electrons to occur, so there is some increase in the triplet binding energy compared to the LSB, but the difference is much less significant than for the singlet.

V. WAVE FUNCTIONS

The calculation yields wave functions for the X^- states, expressed as a set of coefficients for the basis trios used. These can be readily transformed into their full spatial dependence $\psi(r_1,\theta_1,z_1;r_2,\theta_2,z_2;r_h,\theta_h,z_h)$ using the expressions for the basis states in Appendix A. Taking the squared modulus of this wave function and integrating over the remainder of the variables, we calculate single coordinate probability functions, such as $P(r_1)$, and two particle correlation functions of single coordinates, such as $P(r_1,r_2)$. In fact, the two-particle probability $P(r_1,r_2)$ is dominated by the single-particle variations, so the plots show the quantity $P(r_1,r_2)-P(r_1)P(r_2)$, which is a measure of the correlations, in that it would be zero without exchange and correlation effects.

Figures 3 and 4 compare the radial probability functions and electron-electron radial correlation functions for the $M=0$ singlet and $M=-1$ triplet states in the 300-Å well at 20 T. Note that the more negative angular momentum states are degenerate with these states, but their wave functions are not the same, so though similar behavior occurs, these plots are not general.

The difference between the correlation functions for the

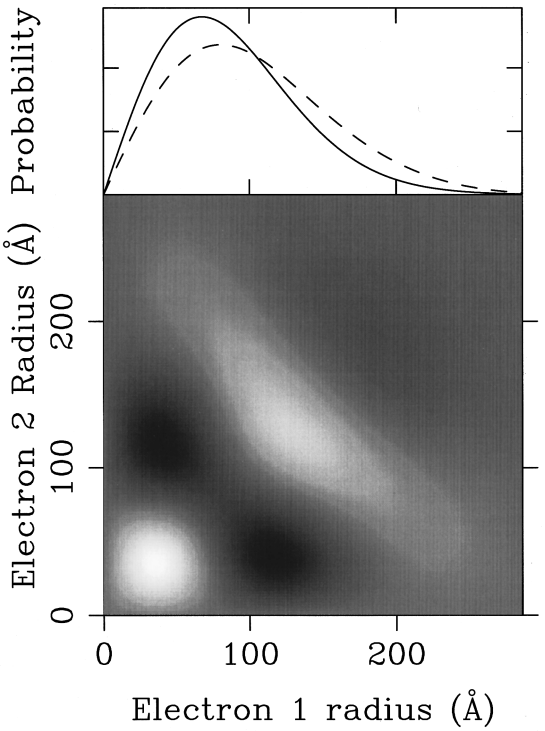

FIG. 3. Upper panel: radial probability functions for electrons (solid lines) and holes (dashed lines) in the $M=0$ singlet state for the 300-Å quantum well at 20 T. Lower panel: radial correlation function for the two electrons; white corresponds to regions of high joint probability, black to regions of low joint probability. See the text for details of the definition of the correlation function.

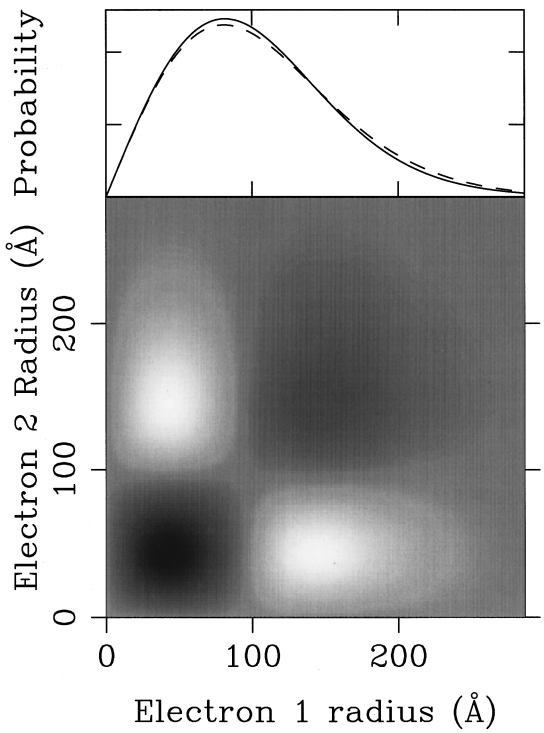

FIG. 4. Radial probability and correlation functions, as in Fig. 3, but for the $M=-1$ triplet state.

two states is very marked. The triplet shows strong anticorrelations between the two electrons: There are low probabilities along the diagonal $r_1=r_2$ and the high probabilities in the regions where the two electrons are at very different radii. The two electrons in the singlet are, by contrast, radially correlated, though the absolute size of the correlations are about two orders of magnitude less than for the triplet (the gray scales on the two figures correspond to different ranges of probabilities). The highest probabilities occur for $r_1=r_2$ and there is relatively low probability of very different radii. Similar effects occur for the angular and axial correlation functions (not shown): In the triplet states the electrons anticorrelate, while in the singlet they correlate. In the axial case, the correlations are much stronger for the singlet than the triplet, as is to be expected from the difference in sensitivity of the two states to the inclusion of the higher subband states in the basis.

The correlation functions illustrate a major difference between the wave functions of the singlet and triplet X^- states. In the singlet, the two electrons tend to stay together, while in the triplet they avoid each other. Ultimately, the explanation for this lies in the different symmetries for electron exchange. The spatially symmetric singlet allows the two electrons to be in the same place, while the antisymmetric triplet forbids it. Given this, it is superficially surprising that the binding energy of the singlet should be so similar to, and even greater than, that of the triplet: The repulsive electron-electron interaction should be much stronger in the singlet than the triplet. The resolution of this puzzle lies in the differences in the attractive electron-hole interaction that these correlations imply. Keeping the electrons together in the singlet allows both to interact strongly with the hole, giving a large electron-hole energy, while the anticorrelations in the triplet prevent both electrons being close to the hole, reducing the electron-hole energy. The total electrostatic contributions to the binding energy, the sum of the positive electron-electron and negative electron-hole parts, thus turn out very similar.

This discussion can be made more quantitative by evaluating the expectation values of the electron-electron and electron-hole Coulomb interactions using the calculated X^- wave functions. In Table III we show the results of this calculation for the 300-Å well at 20 T. The total binding energies given in the table are calculated relative to the Landau-level energies; the exciton binding energy at this field is 15.54 meV. The column marked ''kinetic'' is really just the difference between the electrostatic contribution and the total binding energy. It arises from the inclusion in the wave function of contributions from higher Landau levels and quantum-well subbands. The contrast between the singlet and triplet states is very marked: Though the total binding energies are only ~ 0.3 meV different, the separate electron-electron and electron-hole contributions differ by 3–4 meV.

TABLE III. Contributions to the binding energy (in meV) of the lowest singlet and triplet states in a 300-Å well at 20 T. The binding energy is given relative to the Landau-level energy, rather than X^0, as elsewhere.

X^- state	Electron-electron	Electron-hole	Kinetic	Total
Singlet	10.71	−29.71	2.25	16.75
Triplet	7.44	−25.34	1.42	16.48

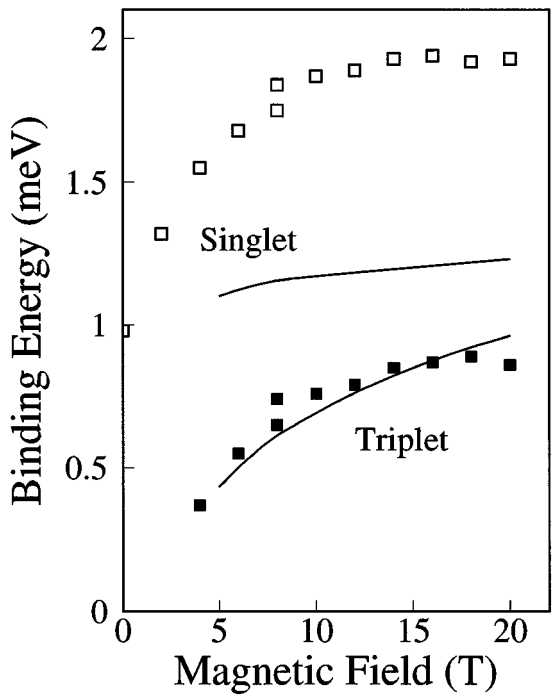

FIG. 5. Comparison between theoretical (lines) and experimental (squares) results for the X^- binding energies in the 300-Å well at fields up to 20 T.

VI. COMPARISON WITH EXPERIMENTS

In this section we compare the best numerical results of Fig. 2 with experimental data for a 300-Å GaAs/$Ga_{0.67}Al_{0.33}As$ quantum well in fields up to 20 T. More details of the experimental structure and procedures are given in Ref. 5. The experimental binding energies are obtained from photoluminescence spectra, which show features due to both X^0 and X^- singlet and triplet recombination. When the X^- recombines, one of the electrons and the hole disappear, leaving a free electron in the lowest Landau level. Thus the difference in photon energies for the X^- and X^0 photoluminescence features is equal to the difference between the energy of the X^- state and the total energy of the X^0 plus a free electron. This is just the X^- binding energy, relative to X^0, that we calculate.

The comparison between theory and experiment is shown in Fig. 5. The agreement we obtain for the triplet states is impressive, considering that no fine-tuning of the physical parameters was required. The situation for the singlet states is much less satisfactory, with the experimental values up to 50% greater than the theory. The calculations do, however, reproduce the very weak field dependence at high fields, despite the actual values being wrong. The disparity for the singlet is much greater than could be explained by incomplete convergence in the calculations, which we estimate to give errors at the level of at most $\sim$0.1 meV. The Monte Carlo results of Ref. 4 appear to give much better agreement than this for the zero field X^-, but this is in part a consequence of the fact that the method requires the use of in-plane masses identical to the axial masses. If the in-plane hole mass is increased to 0.34 in the present calculations, at 10 T the binding energy of the singlet state rises to 1.60 meV much closer to the experimental value of 1.87 meV. The triplet energy, by contrast, changes very little, from 0.69 meV to 0.76 meV, so the agreement remains good. There seems, however, to be no real justification for using such a large value for the in-plane hole mass.

We next discuss some possible reasons for the disparity between the theoretical and experimental values of the singlet binding energy. It is important to note that any suggested explanation for enhancing the singlet binding energy should also account for why the triplet value comes out correctly.

One possibility is that the treatment of the valence band is too simple. The calculations have all assumed that the hole dispersion is parabolic, while in reality this is far from the case. The correct, nonparabolic valence-band dispersion comes from solutions of the Luttinger-Kohn Hamiltonian, coupling together the heavy- and light-hole states. There is some experimental evidence that this may be of importance: In the parabolic model used here, the spin splitting of the X^0 and X^- singlet and triplet states should all be the same. However, experimentally they are different, with a very small splitting for X^0 and larger values for the X^- transitions.[5] Such differences in splitting may be explainable using the Luttinger-Kohn Hamiltonian because states of opposite spin couple in different ways.

We have carried out some calculations[15] using the present approach, but including a proper treatment of the valence band. The main difference is that the hole basis states become a mixture of the simple finite-well states, determined by the Luttinger-Kohn Hamiltonian. The rest of the calculation is then essentially the same, with the electron-hole matrix elements made up of appropriate combinations of the simple finite-well forms derived in Appendix B. The binding energies obtained depend on the values of all the Luttinger parameters, some of which are not accurately known. Various parameter sets have been tried, but the largest singlet binding energy we have been able to obtain is $\sim$1.35 meV at 10 T, still well below the experimental value of 1.87 meV.

A second possibility is that X^- is not free, but in fact bound to a remote donor. This can increase its binding energy relative to X^0 because the latter is neutral and so is much less strongly affected. Taking 600 Å as a reasonable value for the distance of a remote donor from the well, the potential due to a single donor has a depth of $\sim$2 meV. The shift in the X^- photoluminescence line due to this potential is much smaller because the electron left in the final state will also be bound to the donor. Thus the enhancement of the binding energy observed in photoluminescence will only be the difference between the binding energy of the X^- in the donor potential and that of a lone electron. We have obtained theoretical values for this difference using calculations in the lowest subband approximation[15] and found that the singlet is enhanced by $\sim$0.5 meV, while the triplet is virtually unaffected ($<$0.1 meV enhancement). Shifts of this magnitude would give fairly good agreement with the experimental results. The reason for the difference in behavior of the two states is that the correlated electrons in the singlet can interact more strongly with the donor than the anticorrelated electrons in the triplet.

Though this explanation sounds plausible from a theoretical point of view, two pieces of experimental evidence suggest that the observed X^- lines are not donor bound. One reason is that the in-plane donor spacing is sufficiently small

that, at a distance of 600 Å, there must be considerable overlap between the potentials of individual donors, giving rise to a disordered electrostatic potential in the well. Hence the X^- singlet photoluminescence line would be expected to be broader than the X^0 or triplet, by an amount of the order of the singlet enhancement calculated above, about 0.5 meV. This broadening would be easily measurable in the experimental spectra, but no such effect is seen. The other experimental evidence that donor binding is unlikely arises from work on double quantum wells by Shields *et al.*:[16] The binding energy of X^- in one well is measured when there is a large electron density in the other, lying between it and the donors. This would be expected to screen out the donor potential in the well containing X^-. There is, however, no significant dependence of the observed X^- binding energy on the charge density in the other well, suggesting that interactions with donors are unimportant.

A further, more exotic, possibility for explaining the enhancement comes from considerations of the effects of the interaction between the X^- states and photons. Ivanov and Haug[17] have shown that polariton effects can enhance the measured binding energy of a quantum-well biexciton and it seems reasonable to believe that similar effects may occur for X^-. Though no such calculations have been carried out for the X^- system, it is worth pointing out that any such effect would be greater for the singlet than the triplet because the singlet has a much larger oscillator strength and so couples more strongly to the electromagnetic field. Hence this explanation too is consistent with the requirement that the singlet binding energy needs to be enhanced, but not the triplet.

VII. CONCLUSIONS

We have carried out calculations of X^- binding energies in quantum wells with a perpendicular magnetic field. The model consists of a finite width well with finite barrier heights and parabolic conduction and valence bands. Our numerical method is able to cope with large numbers of basis states, allowing us to obtain highly accurate results.

One of the main results of our calculations is to show that the widely used lowest-Landau-level approximation gives poor results for GaAs/$Al_xGa_{1-x}As$ quantum wells, in the range of fields experimentally accessible. Though the LLL predicts that only the triplet X^- state should be bound relative to the neutral exciton X^0, we find that the triplet does not become the ground state until about 30 T in a 100-Å well, while no crossover occurs below 50 T in a 300-Å well. In the latter, correlations perpendicular to the well plane are very important, suggesting that it lies in the crossover regime between two- and three-dimensional behavior. It is clear that the singlet state can only become unbound at much higher fields, perhaps never in the wider well.

The other important result we obtain is an understanding of the different ways that the singlet and triplet states bind. Our correlation functions, and calculations of expectation values, show very clearly that the singlet binds by maximizing the attractive electron-hole interaction, while the triplet minimizes the electron-electron repulsion. This understanding is the key to explaining many of the differences in behavior of the singlet and triplet states.

We believe that our results are very accurate, with numerical errors no more than ~ 0.1 meV. Though good agreement with experiment is obtained for the triplet state, the large discrepancy for the singlet, much greater than this estimated error, suggests that additional physics needs to be considered to understand fully the experimental results.

Finally, we note that since this paper was submitted, Chapman *et al.*[18] have published numerical results for X^- binding energies in a magnetic field. Their approach involves an exact diagonalization within a basis of states from several Landau levels and so is more realistic than previous calculations using only the lowest Landau level. However, when compared to the present work, their treatment has significant limitations with both quantitative and qualitative consequences. The basis they use is too small to obtain high accuracy and indeed no attempt is made to check for convergence. Moreover, they do not include states from higher subbands, which our results show to be very important for even a qualitative understanding of wider wells.

APPENDIX A: SINGLE-PARTICLE WAVE FUNCTIONS

This appendix describes the single-particle electron-hole states for a finite quantum well with a magnetic field perpendicular to its plane. The state factorizes into an axial part $\chi_l(z)$ and an in-plane part $\phi_{nm}(r)\exp\pm i(n-m)\theta$, where the exponent takes opposite signs + and − for electrons and holes, respectively.

For the case of a symmetric, finite quantum well of width d, the axial wave functions can be written in the form

$$\chi_l(z)=\begin{cases} \mathcal{Z}^{\cos}_{\sin}(-kd/2)e^{\alpha z} & (z<-d/2) \\ \mathcal{Z}^{\cos}_{\sin}(kz) & (-d/2<z<d/2) \\ \mathcal{Z}^{\cos}_{\sin}(kd/2)e^{-\alpha z} & (d/2<z), \end{cases} \tag{A1}$$

where the cos form applies for the even-parity states ($l=1,3,\ldots$) and the sin form for odd-parity states ($l=2,4,\ldots$). The normalization constant $\mathcal{Z}$ is given by

$$\mathcal{Z}=\left\{\frac{d}{2}+\frac{1}{2k}\sin kd+\frac{1}{\alpha}\cos^2\frac{kd}{2}\right\}^{-1/2}. \tag{A2}$$

The constants k and α, which, of course, depend on the state l, are determined by numerically solving the trancendental equation derived from the 1D finite-well eigenproblem. In the present work, the boundary conditions used are continuity of χ and $(1/m)\chi'$. The calculations are for a GaAs-$Al_xGa_{1-x}As$ system with $x=0.33$, taking conduction- and valence-band offsets to be 224 and 150 meV, respectively. The electron (hole) masses for axial motion are 0.065 (0.34) and 0.07 (0.45) in the well and barrier and the in-plane values are 0.065 (0.18).

For the in-plane motion, the conventions of MacDonald[19] are followed in choosing the relative phases of the different states. The radial wave functions are then

$$\phi_{nm}(r)=(-1)^{i_<}\frac{e^{-r^2/4l_c^2}}{\sqrt{2\pi l_c^2}}\sqrt{\frac{i_<!}{i_>!}}\left(\frac{r}{\sqrt{2l_c^2}}\right)^{i_>-i_<} \times L_{i_<}^{i_>-i_<}(r^2/2l_c^2), \tag{A3}$$

where L is a generalized Laguerre polynomial and the notation $i_>$ and $i_<$ has been adopted for the greater and lesser of n and m, respectively. This definition is consistent with the phases of the matrix elements in Appendix B.

APPENDIX B: CALCULATION OF COULOMB MATRIX ELEMENTS

This appendix gives details of the analytic part of the evaluation of the Coulomb matrix element coupling pairs of single-particle basis states. In the interests of clarity, the derivation given is just for the electron-electron interaction, minor differences for the electron-hole interaction are mentioned in passing.

The required Coulomb matrix elements take the form

$$\langle l_1 n_1 m_1|\langle l_2 n_2 m_2|V(\mathbf{r}_1-\mathbf{r}_2,z_1-z_2)|l_1' n_1' m_1'\rangle|l_2' n_2' m_2'\rangle, \tag{B1}$$

where

$$V(\mathbf{r}_1-\mathbf{r}_2,z_1-z_2)=\frac{1}{\sqrt{(\mathbf{r}_1-\mathbf{r}_2)^2+(z_1-z_2)^2}}. \tag{B2}$$

Formally evaluating the z integrals, define

$$V_{l_1 l_2 l_1' l_2'}(\mathbf{r}_1-\mathbf{r}_2)$$

$$\equiv\frac{1}{(2\pi)^2}\int\int q\,dq\,d\theta\,\tilde{V}_{l_1 l_2 l_1' l_2'}(q)e^{-i\mathbf{q}\cdot(\mathbf{r}_1-\mathbf{r}_2)}$$

$$=\langle l_1|\langle l_2|V(\mathbf{r}_1-\mathbf{r}_2,z_1-z_2)|l_1'\rangle|l_2'\rangle. \tag{B3}$$

Then the matrix element (B1) can be written

$$\frac{1}{(2\pi)^2}\int\int q\,dq\,d\theta\,\tilde{V}_{l_1 l_2 l_1' l_2'}(q)$$

$$\times\langle n_1 m_1|e^{-i\mathbf{q}\cdot\mathbf{r}_1}|n_1' m_1'\rangle\,\langle n_2 m_2|e^{i\mathbf{q}\cdot\mathbf{r}_2}|n_2' m_2'\rangle. \tag{B4}$$

The next step requires a result due to MacDonald[19] for the Landau-level matrix elements of plane waves. For electrons,

$$\langle nm|e^{-i\mathbf{q}\cdot\mathbf{r}}|n'm'\rangle$$

$$=e^{-q^2 l_c^2/2}G_{n'n}(ql_c)G_{m'm}(ql_c)e^{i(n'-n+m-m')\theta}, \tag{B5}$$

where

$$G_{s's}(ql_c)=\sqrt{\frac{s_<!}{s_>!}}\left(-\frac{iql_c}{\sqrt{2}}\right)^{s_>-s_<}L_{s_<}^{s_>-s_<}(q^2 l_c^2/2). \tag{B6}$$

For holes, the sign of the exponent in the angular part of Eq. (B5) is reversed.

This identity can be used to simplify the matrix elements in Eq. (B4). The θ integral just gives angular-momentum conservation $n_1-m_1+n_2-m_2=n_1'-m_1'+n_2'-m_2'$, leaving a one-dimensional q integral that has to be evaluated numerically:

$$\frac{1}{2\pi}\int\int q\,dq\,\tilde{V}_{l_1 l_2 l_1' l_2'}(q)e^{-q^2 l_c^2}G_{n_1' n_1}(ql_c)G_{m_1' m_1}(ql_c)$$

$$\times G_{n_2' n_2}(-ql_c)G_{m_2' m_2}(-ql_c). \tag{B7}$$

The same result applies for the electron-hole interaction, except the angular-momentum conservation condition correctly becomes $n_e-m_e+m_h-n_h=n_e'-m_e'+m_h'-n_h'$.

In an exactly two-dimensional system, i.e., the limit of zero well width, there are no subband labels and $\tilde{V}(q)=2\pi/q$. In a finite width well, this is multiplied by a form factor $F_{l_1 l_2 l_1' l_2'}(q)$, where

$$F_{l_1 l_2 l_1' l_2'}(q)$$

$$=\int\int dz_1\,dz_2\,\chi_{l_1}(z_1)\chi_{l_1'}^*(z_1)\chi_{l_2}(z_2)\chi_{l_2'}^*(z_2)e^{-q|z_1-z_2|}. \tag{B8}$$

For the case of a finite quantum well with no electric field, this integral can be evaluated analytically. The calculation is lengthy, so only the result is given here.

The finite quantum-well wave functions are described in Appendix A. For each l, the numerical solution gives values of k, the wave vector in the well; α, the decay constant in the barrier; and the normalization constant $\mathcal{Z}$. To keep the expressions for the matrix elements compact, a further quantity p is defined: $p=0$ for even-parity states and $p=1$ for odd-parity states.

The form factors are written in terms of a subsidiary function

$$f(k_a,\alpha_a;k_b,\alpha_b;q)=\frac{1}{k_a^2+q^2}\left(\frac{k_a}{\alpha_b+q}+\frac{q}{k_a+k_b}\right)s^+(k_a,k_b;q)+\frac{1}{k_b^2+q^2}\left(\frac{k_b}{\alpha_a+q}+\frac{q}{k_a+k_b}\right)s^-(k_a,k_b;q)+\frac{1}{(\alpha_a+q)(\alpha_b+q)}$$

$$\times\left(1+\frac{q}{\alpha_a+\alpha_b}\right)c^+(k_a,k_b;q)+\left(\frac{q}{(\alpha_a+q)(\alpha_b+q)(\alpha_a+\alpha_b)}+\frac{q}{(\alpha_b+q)(k_a^2+q^2)}\right.$$

$$\left.+\frac{q}{(\alpha_a+q)(k_b^2+q^2)}-\frac{(q^2+k_a k_b)}{(q^2+k_a^2)(q^2+k_b^2)}\right)c^-(k_a,k_b;q), \tag{B9}$$

where

$$s^\pm(k_a,k_b;q)=\sin(k_a+k_b)d/2\pm e^{-qd}\sin(k_a-k_b)d/2,$$

$$c^{\pm}(k_a,k_b;q)=\cos(k_a+k_b)d/2\pm e^{-qd}\cos(k_a-k_b)d/2. \tag{B10}$$

Then

$$\begin{aligned}F_{l_1l_2l_1'l_2'}(q)=&\frac{\mathcal{Z}_1\mathcal{Z}_2\mathcal{Z}_1'\mathcal{Z}_2'}{4}(-1)^{(p_1+p_2+p_1'+p_2')/2}\\&\times\{f(k_1+k_1',\alpha_1+\alpha_1';k_2+k_2',\alpha_2+\alpha_2';q)+(-1)^{p_2'}f(k_1+k_1',\alpha_1+\alpha_1';k_2-k_2',\alpha_2-\alpha_2';q)\\&+(-1)^{p_2}f(k_1+k_1',\alpha_1+\alpha_1';-k_2+k_2',-\alpha_2+\alpha_2';q)+(-1)^{p_2+p_2'}f(k_1+k_1',\alpha_1+\alpha_1';-k_2-k_2',-\alpha_2-\alpha_2';q)\\&+(-1)^{p_1'}f(k_1-k_1',\alpha_1-\alpha_1';k_2+k_2',\alpha_2+\alpha_2';q)+(-1)^{p_1'+p_2'}f(k_1-k_1',\alpha_1-\alpha_1';k_2-k_2',\alpha_2-\alpha_2';q)\\&+(-1)^{p_1'+p_2}f(k_1-k_1',\alpha_1-\alpha_1';-k_2+k_2',-\alpha_2+\alpha_2';q)\\&+(-1)^{p_1'+p_2+p_2'}f(k_1-k_1',\alpha_1-\alpha_1';-k_2-k_2',-\alpha_2-\alpha_2';q)\}.\end{aligned} \tag{B11}$$

Note that the full result has sixteen terms, corresponding to all possible combinations of signs. This form of it has been simplified by combining pairs of terms in a way that is valid only for parity-allowed matrix elements. It thus does not correctly give zero for the parity-forbidden case.

A useful special case that can be derived from Eqs. (B9)–(B11) is the diagonal lowest subband ($l=1$) form factor for an infinite well ($k=\pi/d$, $\alpha\to\infty$). Then, as in Ref. 20,

$$F_{1111}(q)=\frac{2}{qd}+\frac{qd}{q^2d^2+4\pi^2}-2(1-e^{-qd})\left(\frac{1}{qd}-\frac{qd}{q^2d^2+4\pi^2}\right)^2. \tag{B12}$$

[1] M. A. Lampert, Phys. Rev. Lett. **1**, 450 (1958).

[2] A. J. Shields, C. L. Foden, M. Pepper, D. A. Ritchie, M. P. Grimshaw, and G. A. C. Jones, Superlattices Microstruct. **15**, 355 (1994); A. J. Shields, M. Pepper, D. A. Ritchie, M. Y. Simmons, and G. A. C. Jones, Phys. Rev. B **51**, 18 049 (1995).

[3] G. Finkelstein, H. Shtrikman, and I. Bar-Joseph, Phys. Rev. Lett. **74**, 976 (1995).

[4] A. J. Shields, F. M. Bolton, M. Y. Simmons, M. Pepper, and D. A. Ritchie, Phys. Rev. B **55**, R1970 (1997).

[5] A. J. Shields, M. Pepper, M. Y. Simmons, and D. A. Ritchie, Phys. Rev. B **52**, 7841 (1995).

[6] D. C. Mattis, in *The Theory of Magnetism* (Springer-Verlag, Berlin, 1981), Vol. 1, p. 106.

[7] B. Stebe and A. Ainane, Superlattices Microstruct. **5**, 545 (1989).

[8] J. L. Osborne, A. J. Shields, M. Pepper, F. M. Bolton, and D. A. Ritchie, Phys. Rev. B **53**, 13 002 (1996).

[9] B. Stébé, A. Ainane, and F. Dujardin, J. Phys.: Condens. Matter **8**, 5383 (1996).

[10] B. Stébé, E. Feddi, and G. Munschy, Phys. Rev. B **35**, 4331 (1987).

[11] A. Wojs and P. Hawrylak, Phys. Rev. B **51**, 10 880 (1995).

[12] J. J. Palacios, D. Yoshioka, and A. H. MacDonald, Phys. Rev. B **54**, R2296 (1996).

[13] For the singlet, if the quantum numbers of the two electrons are identical, the factor $1/\sqrt{2}$ has to be replaced by 1/2 to give the correct normalization.

[14] H. L. Fox and D. M. Larsen, Phys. Rev. B **51**, 10 709 (1995).

[15] D. M. Whittaker (unpublished).

[16] A. J. Shields, J. L. Osborne, D. M. Whittaker, M. Y. Simmons, M. Pepper, and D. A. Ritchie, Phys. Rev. B **55**, 1318 (1997).

[17] A. L. Ivanov and H. Haug, Nuovo Cimento D **17**, 1255 (1995).

[18] J. R. Chapman, N. F. Johnson, and V. N. Nicopoulos, Phys. Rev. B **55**, R10 221 (1997).

[19] A. H. MacDonald, in *Mesoscopic Quantum Physics*, edited by E. Akkermans, G. Montambaux, J.-L. Pichard, and J. Zinn-Justin (Elsevier Science, Amsterdam, 1995), pp. 659–720.

[20] P. Hawrylak, Solid State Commun. **88**, 475 (1993).